Influence of Using Different Segmentation Methods on the Fractal Properties of the Identified Retinal Vascular Networks in Healthy Retinas and in Retinas with Vein Occlusion

Zoltán Fazekas[1], András Hajdu [2], István Lázár[2], György Kovács[2], Béla Csákány[3], Dan Mihai Călugăru[4], Rajiv Shah[5], Ema I. Adam[6], and Ştefan Ţălu[7]

[1] Institute for Computer Science and Control (MTA SZTAKI), Systems and Control Laboratory, H-1111 Kende u. 13-17, Budapest, Hungary
[2] University of Debrecen, Department of Computer Graphics and Image Processing, H-4028, Debrecen, Kassai út 26.
[3] Semmelweis University, Faculty of Medicine, Department of Ophthalmology, H-1085 Mária u. 39, Budapest, Hungary
[4] Iuliu Haţieganu University of Medicine and Pharmacy, Faculty of Medicine, Dept. of Surgical Specialties and Medical Imaging, Discipline of Ophthalmology, RO-400012 8 Victor Babeş St., Cluj, Romania
[5] Wayne State University, School of Medicine, Kresge Eye Institute, Vitreoretinal Surgery and Uveitis and Ocular Immunology, 4717 St. Antoine Detroit, MI 48201, USA
[6] Technical University of Cluj-Napoca, Faculty of Machine Building, Dept. of Modern Languages and Communication, RO-400641 103-105 B-dul Muncii St., Cluj, Romania
[7] Technical University of Cluj-Napoca, Faculty of Mechanical Engineering, Dept. of AET, Discipline of Descriptive Geometry and Engineering Graphics, RO-400641 103-105 B-dul Muncii St., Cluj, Romania.

Abstract. Two recent retinal blood vessel (RBV) segmentation algorithms were evaluated on fundus images taken of healthy retinas and retinas affected by retinal vein occlusion (RVO) in a pilot study intended to lead firstly towards a joint disease-specific segmentation algorithm evaluation effort, and secondly, to setting up a comprehensive RBV segmentation palette and knowledge-base. In the pilot study, overall fractal properties of segmented RBV networks were computed and compared. For segmentation, the aforementioned two algorithms were used. Based on our results, the fractal properties of the identified RBV networks are seen as promising in quantifying the pathological stages and the types of RVO. Our results suggest that both considered segmentation algorithms lead to usable RBV segmentations.

Keywords: Computer-aided medical diagnosis systems. Retinal blood vessel segmentation algorithms; Retinal vein occlusion; Fractal analysis;

1 Introduction

The shape and the morphological characteristics of patients' retinal vascular networks – as seen via some viewing device by ophthalmologists, or as imaged using various

imaging modalities with ophthalmic diagnostic devices during examinations – convey a wealth of eye- and sight-related diagnostic information, as well as general diagnostic information to ophthalmologists about their patients [1] and [2].

This information can be extracted, processed and utilized by computer-based diagnosis and measurement systems to produce quantitative diagnostic data that facilitate the medical diagnosis [3]. Nowadays, the quantitative analysis of the retinal vascular networks is mostly carried out by multi-stage diagnosis software – [4] and [5] – incorporated in computer-based diagnosis and measurement systems. The identification – i.e., segmentation – of the retinal vascular network is carried out in one of the first stages of the analysis.

Improving blood vessel segmentation methods used for the purpose is a prime target of intensive research and experimentation. The invested research effort is indicated by the large number of publications by the members of the medical imaging community [6]. Some concrete retinal blood vessel (RBV) segmentation methods and their diagnostic utility will be touched upon in Subsection 1.2.

In the present paper, certain overall fractal properties of vascular networks found – and imaged in vivo with fundus cameras – in healthy retinas and in retinas with vein occlusion are computed and compared. Fractal analysis concepts and fractal-based approaches used in the characterisation of retinal vascular networks are touched upon in Subsections 1.3 and 1.4, respectively.

For the identification of the branching image regions – within the images taken with the fundus cameras – corresponding to the retinal vascular networks, i.e., to produce the vascular binary maps, or in other words, for the RBV segmentation, the algorithms outlined in Subsections 2.1 and 2.2, respectively, were used.

Many known pathologies change the morphological characteristics of the retinal vascular networks considerably, see e.g., [7] through [9], [35] and [39]. One of these is the retinal vein occlusion (RVO) disease. RVO is a frequent cause of visual loss, particularly amongst older people. RVO retinas were chosen – for the purpose of this evaluation –as an archetype of the vascular morphological change. RVO is briefly described and categorised in Subsection 1.1.

The evaluation presented herein should be seen as part of a comprehensive disease-specific vascular segmentation algorithm evaluation effort that is expected to establish a disease-specific RBV segmentation palette and a related knowledge-base. This specialized palette will enhance and will be used in conjunction with the generic RBV segmentation methods known from the literature.

1.1   Retinal vein occlusion

Retinal vein occlusion (RVO) is an important cause of visual loss among older adults throughout the world [10]. This condition is the second most common cause of vision loss amongst the cases directly related to some retinal vascular disease (with diabetic retinopathy being the most common one).

RVO is classified according to where the obstruction appears. Obstruction of the retinal vein at the optic nerve is referred to as central RVO, while obstruction at a branch of the retinal vein is referred to as branch RVO. These forms have many

differences and many commonalities in their pathogenesis and in their clinical presentation [11].

Despite many proposed medical interventions, there are no treatments known to reopen occluded retinal veins in the clinical practice [12]. Treatments are, therefore, aimed at the secondary, vision-threatening complications of this condition. These complications include macular edema, retinal neovascularization, and anterior segment neovascularization.

1.2 Retinal Blood Vessel Segmentation Methods

Automatic identification and analysis of retinal vasculature, see e.g., [13] through [18], can assist medical personnel with repeatable quantification of vascular features [19] and [20], lesion detection [21] and [22], establishing links between retinal and cerebral vasculature [23], and modelling the variability of clinical judgement [24]. Unsupervised methods known from the literature are based on matched filters [25], grouping of edge pixels [26], adaptive thresholding [27], vessel tracking [28] and morphological techniques [7], [29], [30] and [46].

Further methods are cited in Subsections 2.1 and 2.2 in conjunction with the concrete RBV segmentation methods used herein.

1.3 Fractal analysis concepts

In fractal analysis, the box-dimension – computed via the box-counting – is the most common method used to estimate the fractal dimension. The lower and upper box-counting dimensions of a subset, respectively, are defined in [50][1] as follows:

$$\underline{\dim}_B(F) = \varliminf_{\delta \to 0} \frac{\log N_\delta(F)}{-\log \delta}; \qquad \overline{\dim}_B(F) = \varlimsup_{\delta \to 0} \frac{\log N_\delta(F)}{-\log \delta} \tag{1}$$

If the lower and upper box-counting dimensions are equal, then their common value is referred to as the box-counting dimension of F and is denoted with

$$\dim_B(F) = \lim_{\delta \to 0} \frac{\log N_\delta(F)}{-\log \delta} \tag{2}$$

where $N_\delta(F)$ can be of the following: (i) the smallest number of closed "balls" (i.e., disks, spheres) of radius $\delta > 0$ that cover F; (ii) the smallest number of cubes of side δ that cover F; (iii) the number of δ-mesh cubes that intersect F; (iv) the smallest

---

[1] There are numerous examples and applications related to fractal analysis in the cited book. The book features numerous instructive figures and diagrams that help to grasp the meaning of fractal analysis concepts and methodology.

number of sets of diameter at most δ that cover F; (v) the largest number of disjoint "balls" of radius δ with centres in F.

In practice, the fractal analysis relies on the experimental and methodological parameters related to diversity of objects, homogeneity of the image acquisition, types of images considered, whether further processing is required, or not.

1.4 Fractal Properties of the Retinal Vascular Networks

The morphogenesis of the human retinal vascular network can be modelled as a diffusion-limited aggregation process [31]. The structures produced by such processes appear in apparently unrelated areas. In many cases, these areas are connected only by the common diffusion processes working in the background.

The diffusion-limited aggregation processes tend to build up branching structures exhibiting fractal characteristics (e.g., self-similarity at low resolutions) [32]. According to investigations reported in [31] and [33], the fractal dimension of the vascular network in a healthy human retina is about 1.7.

Among the morphological methods utilized in ophthalmic measurements and diagnosis for detecting and segmenting the vascular network of the human retina – these include the methods referred to in Subsection 1.2 – various fractal-based methods were also applied for the purpose, e.g., [34] and [35]. Such methods were used in the detection, the description and the diagnosis of various vascular and non-vascular pathological conditions, see [35] and [36].

Despite the agreement concerning the fractal dimension of healthy retinas, there is no consensus regarding the fractal dimensions of vascular networks in human retinas affected by particular pathological disorders, see [35] through [38].

The human retinal vascular network was also found to have a multifractal morphological structure [22] and [39]. Similarly to the wider known fractal analysis, multifractal analysis was applied to the assessment of the branching geometry and the pattern complexity, and for quantifying and detecting retinal vascular diseases and symptoms [8] and [37].

2 Segmentation methods evaluated in this study

As it was stated in the Introduction, two recent methods were used in the pilot study presented herein for the purpose of RBV segmentation in retinal fundus images.

2.1 Method A

In this subsection, the first of the methods mentioned above will be outlined. For simplicity, this method will be referred to as method A. The method was proposed and is fully described in [40], herein it is summarised for the readers' convenience.

Method A is a RBV segmentation method that produces a vascular binary map of the retinal fundus image used as input. It makes use of directional response vector

similarity and carries out region growing. While there are many directional and multiscale methods known from the literature, the manner in which the directional responses are used in method A distinguishes it from the state-of-the-art. For instance, many RBV segmentation methods – including [41] through [43] – rely on either the maximal, or some aggregated (e.g., summed, or averaged) responses to directional 2D filters at each pixel; on the other hand, method A, as well as the method proposed in [44], store and handle all the directional responses in a vector for each pixel.

Method A is in essence a purpose-made region growing procedure – making use of the well-known hysteresis thresholding technique – applied to the response vector similarities of adjacent pixels within the fundus image.

During processing an RBV score map is created and used by the method. The score map is a pixelwise combination of various statistical measures of the response vectors. The local maxima of the score map provide seeds for the region growing procedure. A nearest neighbour classifier – based on a rotation-invariant response vector similarity measure – is used to eliminate uncertain seed points.

Many techniques that capture the Gaussian-like cross-section of blood vessels give high responses to the abrupt intensity transitions at the boundary of the optic disc and bright lesions. To overcome this drawback, method A applies a symmetry-constrained multiscale matched filtering technique.

The correlation-based similarity metric for directional response vectors and the classifier setup used in method A are novel in the field of retinal image analysis, while its region growing scheme could well be used in other application fields, as well.
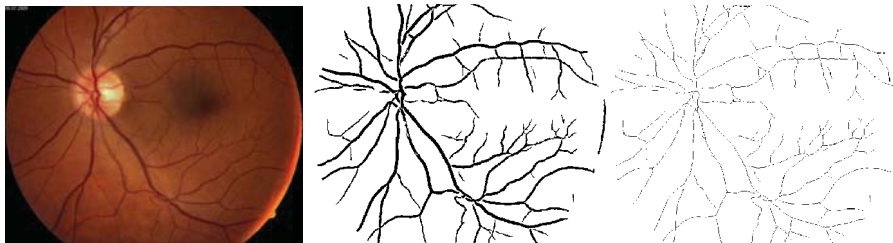

Fig. 1. Retinal fundus image of a left eye with normal blood vessel network. From left to right: the original image, the segmented image and its skeletonised version. For the vascular segmentation, method A was used.

Method A was tested on the publicly available DRIVE [51] and STARE [52] retinal image sets. The experimental results presented in [40] show that its sensitivity – particularly at the diagnostically important low false-positive rates – is close to that of a human observer, and is competitive with that of other state-of-the-art vessel segmentation techniques.

The method is computationally effective, and therefore well-suited for real-time computer-aided diagnosis applications. It is particularly so, if the host computer system is equipped with appropriate parallel computing resources, as the computationally most critical processing steps of the method are implemented with a view on parallel execution.

2.2 Method B

The second RBV segmentation method used and evaluated herein – again producing a binary blood vessel map for the input fundus image – is described fully in [45]. The method will be referred to as method B in the rest of the paper. It is summarised in this subsection to make the paper more readable and standalone.

Method B is based on directional response vector similarity and region growing. The response vector is calculated via template matching carried out with generalized forms of Gabor functions. Unlike other methods that use matched Gabor filtering with only a few specific Gabor filters, e.g., the method proposed in[15], method B relies on a large set of such templates in modelling various parts of the retinal vascular system.

A number of novel solutions were used in method B. Firstly, in order to reconstruct the original distribution of vessel widths, the results of the individual template matching and region growing steps are unified. Secondly, the problem of false RBV detections near bright lesions and other bright areas is explicitly addressed. Thirdly, the edges of the raw segmentation results are refined to mimic the local characteristics of blood vessel edges identified manually. Furthermore, method B explicitly addresses the issue of thin vessels.

Due to these novel solutions, method B outperforms the majority of published methods in respect of the widely used public retinal image-bases, and features better RBV segmentations – on average – than the second best (non-expert) human operator in respect of the mentioned image-bases.
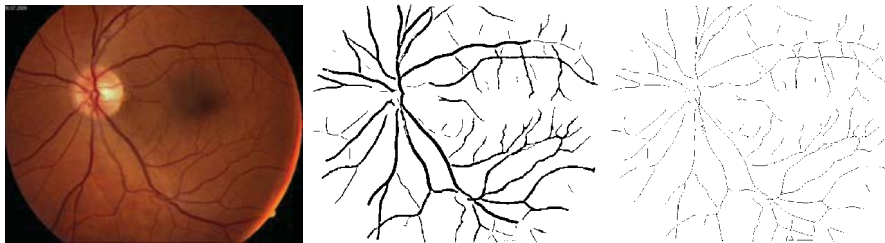

Fig. 2. The retinal image – same as the one shown in Fig. 1 – is segmented and skeletonized. For the vascular segmentation, method B was used.

For the quantitative evaluation presented in [51], the method was trained on images from the DRIVE database – the only public database that has a well-specified training set – and was evaluated on the test images of the database, as well as on all the images of the STARE [52] and HRF [53] databases. Even though the images of the latter databases were taken by different devices and under various circumstances, furthermore, they differ in size from the training images, the results achieved by method B are competitive with that of other techniques trained and evaluated on disjoint subsets of the latter databases.

Method B is fairly robust against unexpected inputs. This feature makes method B a possible building block of retinopathy screening systems. On the other hand, its

novel solutions can be integrated into other existing vessel segmentation methods to improve their accuracy.

3 Evaluation of the Methods

In this section, the retinal fundus images used in the evaluation, the details of the evaluation procedure, the results gained from it and the discussion of the results are presented.

3.1 Images used in the evaluation

The fundus images presented here were taken of retinas of patients – with their explicit and informed consent – treated at the Ophthalmological Clinic in Cluj-Napoca in 2009. The images were anonymised by the authorized personnel of the clinic as part of a pharmacological research project concentrating on acute central and hemi-central RVO's [47]. The images were captured by a Zeiss VISUCAM fundus camera using a 45° field-of-view.

3.2 Evaluation procedure

Fractal analysis was performed in conjunction with the segmented images and their skeletonized versions of a number of retinal images taken as explained in the previous subsection.
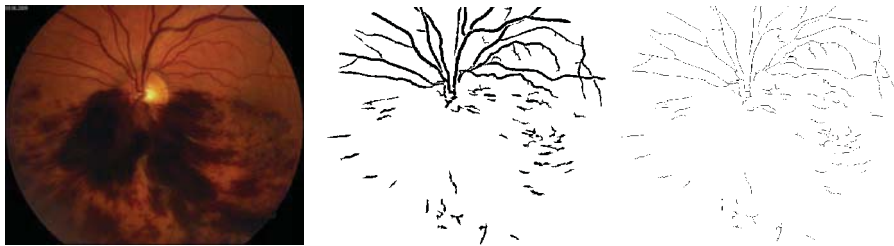

Fig. 3. Retinal fundus image of an eye affected by hemi-central RVO. From left to right: the original image, the segmented image and its skeletonized version. For the vascular segmentation, method A was used.

The retinal images presented herein correspond to a healthy cornea (Figs. 1 and 2) and to corneas affected by different types of the RVO disease (Figs. 3 - 8). For each cornea, the original image, its segmented versions (i.e., version 1: segmented using method A, and version 3: segmented with method B) and its skeletonised versions (i.e., version 2: the original image segmented with method A and skeletonised thereafter, and version 4: the same image segmented with method B and skeletonised

thereafter) are presented. The fractal analysis of the segmented/skeletonized images was carried out using the box-counting algorithm, which was explained in Subsection 1.3. The skeletonising was accomplished and fractal dimensions of the identified retinal vascular networks were computed with the Image J software [48] augmented with the FracLac plug-in [49]. The fractal dimensions computed for the identified (i.e., segmented, or skeletonized) retinal vascular networks are collated in Table 1.
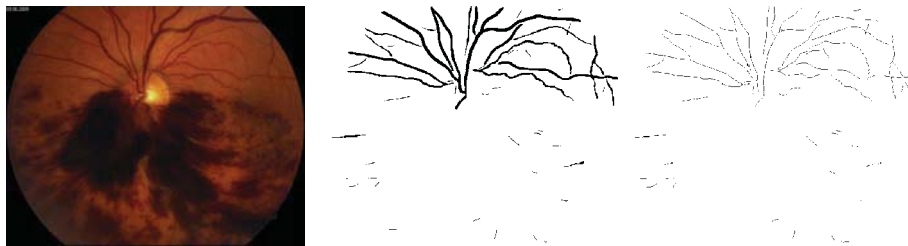

Fig. 4. The retinal image – same as the one shown in Fig. 3 – is segmented and skeletonized. For the vascular segmentation, method B was used.

For the fractal analysis, the following options and settings were used in conjunction with the aforementioned software configuration: a) 10 grid positions were used; b) grid calibers were computed using default box sizes. The range of box-sizes used for the fractal dimension calculation was between 2 pixels and 45 % of the length corresponding to the shorter side of the region-of-interest.

Table 1. The fractal dimensions computed for the identified (segmented or skeletonized) retinal vascular networks shown in Figs. 1-8.

	Segmented with method A	Skeletonized version (for method A)	Segmented with method B	Skeletonized version (for method B)
Normal retina shown in Figs. 1 & 2	**1.6048**	1.5185	**1.5998**	1.4973
Hemicentral RVO retina shown in Figs. 3 & 4	**1.4741**	1.4299	**1.3768**	1.2961
Central RVO retina shown in Figs. 5 and 6	**1.5790**	1.5385	**1.4469**	1.3637
Branch RVO retina shown in Figs. 7 and 8	**1.5806**	1.5243	**1.4852**	1.4074

3.3   Results and Discussion

The images presented herein were selected from a considerably larger set of images (see detail in Subsection 3.1) by our ophthalmologist co-authors. No manual RBV segmentation of the images has been carried out due to time limitations. Therefore, at this stage we cannot compare the computed fractal dimensions presented in Table 1 to that of the RBV segmentations created by experts. What we can still do is to take these values as morphological features characterising retinas either affected, or not by certain RVO and look at how well these values separate the cases considered.

As in other papers presenting fractal analysis results for retinal vascular networks, see e.g., [34] through [38], both the segmented and skeletonized images are processed and evaluated.

The fractal dimensions of skeletonised RBV network tend to be lower than that of the corresponding segmented networks (which have not been skeletonised). This rule-of-thumb holds also for the fractal dimensions presented in Table 1. It is therefore more interesting to look at the differences showing up in the fractal dimensions of RBV network identified with different algorithms (i.e., by the methods A and B).
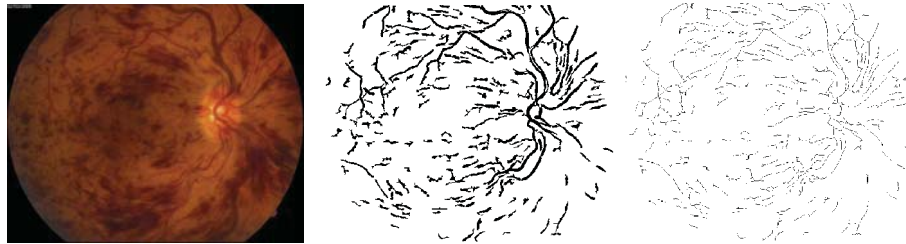

Fig. 5. Retinal fundus image of an eye affected by central RVO of non-ischemic type. From left to right: the original image, the segmented image and its skeletonized version. For the vascular segmentation, method A was used.

Fig. 6. The retinal image – same as the one shown in Fig. 5 – is segmented and skeletonized. For the vascular segmentation, method B was used.

Clearly, there is no significant difference in fractal dimensions – computed for the retinal images segmented by methods A and B – in case of the presented healthy

retina. There are, however, perceivable differences present in case of retinas affected by RVO. The biggest difference in fractal dimension is for the retina – shown in Figs. 5 and 6 – affected by central RVO. Similar tendencies can be identified both for the segmented and the skeletonised corneas, therefore, it does not really matter whether one looks at the corresponding segmented RBV networks (segmented by methods A and B, respectively), or at the corresponding skeletonised networks (which had been segmented earlier by methods A and B, respectively). So, for example, the biggest difference in fractal dimension occurs for the same retina (i.e., the one affected by central RVO) if one considers the skeletonised versions of the images.
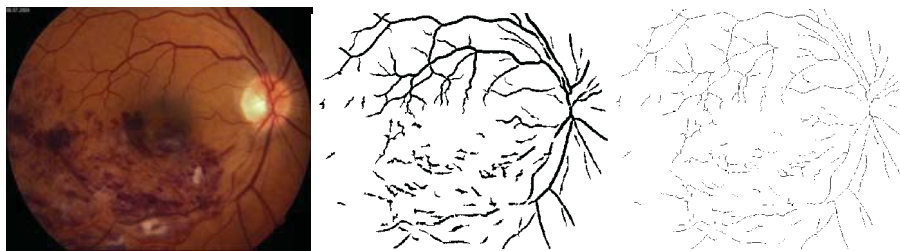

Fig. 7. Retinal fundus image of an eye affected by branch RVO. From left to right: the original image, the segmented image and its skeletonized version. For the vascular segmentation, method A was used.
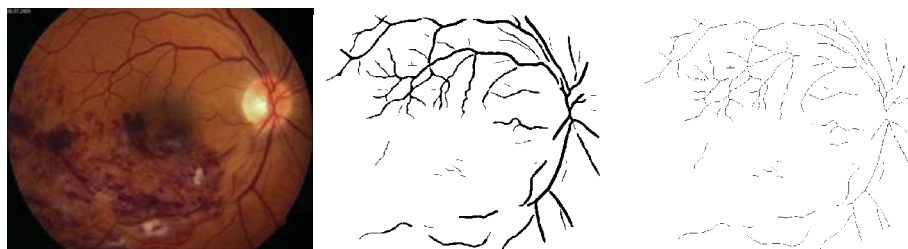

Fig. 8. The retinal image – same as the one shown in Fig. 7 – is segmented and skeletonized. For the vascular segmentation, method B was used.

The fractal dimensions computed as detailed above seem to be useful in separating the various types of RVO. In this respect, method B performs better than method A does (at least in respect of the retinal images considered and presented herein), as the former method produces a wider gap between the fractal dimension of the central RVO retina's RBV network (see Fig. 6) and that of the branch RVO retina's RBV network (see Fig. 8) than the latter method does between the fractal dimensions of the corresponding RBV networks, i.e., the ones presented in Figs. 5 and 7, respectively.

In our view, a regional approach – such as used and presented in [39] – would considerably improve the quality of the characterization in respect of the various

stages and the various types of the RVO, and would ensure a better separability between these stages and types.

Further improvement could be achieved in the above characterisation using multifractal-based approaches, such described in [8], [37] and [39] in conjunction with other eye conditions. Such approaches could work well, as the RBV networks can be – and in case of the RVO images presented herein clearly they are – morphologically very inhomogeneous.

4 Conclusions

In the paper, two recent RBV segmentation algorithms were evaluated on fundus images taken of healthy retinas and retinas affected by RVO. As no manual RBV segmentation of the images was carried out, only the vascular maps produced by the two RBV segmentation algorithms outlined in Subsection 2.1 and 2.2, respectively, were used. Both algorithms lead to usable RVB segmentations. The overall fractal dimensions of the segmented RBV networks were computed and compared.

The fractal dimensions seem to be useful in quantifying the types of RVO. In this respect, method B performs better than method A does (at least in respect of the retinal images considered and presented herein). The small number of cases considered, however, prevents statistical conclusions. Nevertheless, the presented cases and results suggest that an evaluation involving a much larger data set of images of retinas affected with RVO is definitely worth doing. Such an extended evaluation should cover both the various stages and the various types of RVO and make use of RBV segmentation created by experts.

In our view, a regional approach would definitely improve the quantification and separability of the RVO cases. Also, the multifractal-based characterisation should be utilized for the purpose, as the RBV network can be morphologically very inhomogeneous, particularly in case of RVO cases.

The presented investigation is meant to contribute towards and lead to the joint disease-specific RBV segmentation algorithm evaluation effort. This joint effort should result in an accepted disease-specific RBV segmentation palette and a related knowledge-base.

References

1. Joshi, V. S.: Analysis of Retinal Vessel Networks Using Quantitative Descriptors of Vascular Morphology. PhD thesis, University of Iowa, IA, 1--182 (2012)
2. Hasan, T., Sharma, S., Asthana, A., Khare, S., Jain, S.: Retinal Microvascular Signs In Adults with Hypertension: Systemic Associations and Risk Reduction, The Internet Journal of Cardiology, 11, (2013)
3. Li, X., Wee, W. G.: Retinal Vessel Detection and Measurement for Computer-Aided Medical Diagnosis. Journal of Digital Imaging. 27,:120--132 (2014)
4. Ţălu, Ş.: Characterization of Retinal Vessel Networks in Human Retinal Imagery Using Quantitative Descriptors. Human & Veterinary Medicine – Bioflux, 5, 5--57 (2013)

5. Fraz, M. M., Remagnino, P., Hoppe, A., Uyyanonvara, B., Rudnicka, A. R., Owen, C. G., Barman, S. A.: Blood Vessel Segmentation Methodologies in Retinal Images – A Survey. Computer Methods and Programs in Biomedicine, 108, 407--433 (2012)

6. Patton, N., Aslam, T. M., MacGillivray, T., Deary, I. J., Dhillon, B., Eikelboom, R. H., Kanagasingam Yogesan, Constable, I. J.: Retinal Image Analysis: Concepts: Applications and Potential. Progress in Retinal and Eye Research, 25, 99--127 (2006)

7. Mendonça, A. M., Campilho, A.: Segmentation of Retinal Blood Vessels by Combining the Detection of Centerlines and Morphological Reconstruction. IEEE Transactions on Medical Imaging, 25, 1200--1213 (2006).

8. Ţălu, Ş: Multifractal Geometry in Analysis and Processing of Digital Retinal Photographs for Early Diagnosis of Human Diabetic Macular Edema. Current Eye Research, 38, 781--792. (2013)

9. Ţălu, Ş, Fazekas, Z., Ţălu, M. and Giovanzana, S.: Analysis of Human Peripapillary Atrophy Using Computerised Image Analysis, Proceedings of 9.th Conference of KEPAF, Bakonybél, Hungary, 427--438 (2013)

10. Rogers, S., McIntosh, R. L., Cheung, N., Lim, L., Wang, J. J., Mitchell, P., Kowalski, J. W., Nguyen, H., Wong T. Y.: The Prevalence of Retinal Vein Occlusion: Pooled Data from Population Studies from the United States, Europe, Asia, and Australia. Ophthalmology, 117, 313--9 (2010)

11. Kolar, P.: Risk Factors for Central and Branch Retinal Vein Occlusion: A Meta-Analysis of Published Clinical Data. Journal of Ophthalmology, Article ID 724780, 1--5, (2014)

12. Madhusudhana, K., C., Newsom, R. S.: Central Retinal Vein Occlusion: the Therapeutic Options. Canadian Journal of Ophthalmol*ogy,* 42, 193--5 (2007)

13. Lowell, J., Hunter, A., Steel, D., Basu, A., Ryder, R., Kennedy, R. L.: Measurement of Retinal Vessel Widths from Fundus Images Based on 2-D Modelling. IEEE Transactions on Medical Imaging, 23, 1196--1204 (2004)

14. Niemeijer, M., Staal, J., van Ginneken, B., Loog, M., Abrmoff, M..D.:Comparative Study of Retinal Vessel Segmentation Methods on a New Publicly Available Database. SPIE Medical Imaging, 5370, 648--656 (2004)

15. Soares, J. V. B., Leandro, J. J. G. Cesar, R. M., Jelinek, H. F., Cree, M. J.: Retinal Vessel Segmentation Using the 2-D Gabor Wavelet and Supervised Classification. IEEE Transactions on Medical Imaging, 25, 1214--1222 (2006).

16. Sofka, M., Stewart, C.V. Retinal Vessel Centerline Extraction Using Multiscale Matched Filters, Confidence and Edge Measures. IEEE Transactions on Medical Imaging, 25, 1531--1546 (2006)

17. Wang, L., Bhalerao, A., Wilson, R.: Analysis of Retinal Vasculature Using a Multiresolution Hermite Model. IEEE Transactions on Medical Imaging, 26, 137--152 (2007)

18. Mahadevan, V., Narasimha-Iyer, H., Roysam, B., Tanenbaum, H. L.: Robust Model-Based Vasculature Detection in Noisy Biomedical Images. IEEE Transactions on Information Technology in Biomedicine, 8, 360--376 (2004)

19. Chapman, N., Witt, N., Gao, X., Bharath, A. A., Stanton, A. V., Thom, S. A., Hughes, A. D.: Computer Algorithms for the Automated Measurement of Retinal Arteriolar Diameters. British Journal of Ophthalmology, 85, 74--79 (2001)

20. Azegrouz, H., Trucco, E., Dhillon, B., MacGillivray, T., MacCormick, I. J.: Thickness Dependent Tortuosity Estimation for Retinal Blood Vessels. Proc. of 28th IEEE International Conference on Engineering in Medicine and Biology, New York, USA, 4675-4678 (2006)

21. Trucco, E., Buchanan, C. R., Aslam, T., Dhillon, B.: Contextual Detection of Ischemic Regions in Ultra-wide-field-of-view Retinal Fluorescein Angiograms. Proc. 29th IEEE International Conference on Engineering in Medicine and Biology, Lyon, France, 6740--6743. (2007)

22. Stosic, T., Stosic, B.: Multifractal Analysis of Human Retinal Vessels. IEEE Transactions on Medical Imaging, 25, 1101--1107 (2006)
23. Patton, N., Patti, A., MacGillivray, T., Aslam, T., Dhillon, B., Gow, A., Starr, J..M., Whalley, L. J., Deary, I. J.: The Association between Retinal Vascular Network Geometry and Cognitive Ability in an Elderly Population. Investigative Ophthalmology and Visual Science, 48, 1995--2000 (2007)
24. Friedman, C. P., Wyatt, J. C.: Evaluation Methods in Biomedical Informatics. Springer, Berlin, Germany, (2006)
25. Hoover, A., Kouznetsova, V., Goldbaum, M.: Locating Blood Vessels in Retinal Images by Piece-wise Threshold Probing of a Matched Filter Response. IEEE Transactions on Medical Imaging, 19,:203--210 (2000)
26. Pinz, A., Berngger, S., Kruger, A.: Mapping the Human Retina. IEEE Transactions on Medical Imaging, 17, 606--619 (1998)
27. Jiang, X., Mojon, D.: Adaptive Local Thresholding by Verification-based Multithreshold Probing with Application to Vessel Detection in Retinal Images. IEEE Transactions on Pattern Analysis and Machine Intelligence, 25, 131--137 (2003)
28. Can, A., Shen, H., Turner, J. N., Tanenbaum, H. L., Roysam, B.: Rapid Automated Tracing and Feature Extraction from Retinal Fundus Images Using Direct Exploratory Algorithms. IEEE Trans on Information Technology in Biomedicine, 3, 1--15 (1999)
29. Zana, F., Klein, J. C.: Segmentation of Vessel-like Patterns Using Mathematical Morphology and Curvature Evaluation. IEEE Transactions on Image Processing, 10, 1010--1019 (2001)
30. Miri, M. S., Mahloojifar, A.: Retinal Image Analysis Using Curvelet Transform and Multistructure Elements Morphology by Reconstruction IEEE Transactions on Biomedical Engineering, 58, 1183--1192 (2011)
31. Masters, B. R.: Fractal Analysis of the Vascular Tree in the Human Retina. Annual Review of Biomedical Engineering, 6, 427--452 (2004)
32 Fazekas, Z.: Graph-based Description of Retinal Blood-vessels in Fluorescein Angiograms. Proceedings of 4th International Workshop on Systems, Signals and Image Processing, Poznan, Poland, 235--238 (1997)
33. Kyriacos, S., Nekka, F., Vicco, P., Cartilier, L.: The Retinal Vasculature: Towards an Understanding of the Formation Process. In: Fractals in Engineering - From Theory to Industrial Applications, Vehel, L. J., Lutton, E., Tricot, G. (Eds.), Springer-Verlag, Berlin, 383--397 (1997)
34. Mendonça, M. B., Garcia, C. A. A., Nogueira, R. A., Gomes, M. A., Valença, M. M., Oréfice, F.: Fractal Analysis of Retinal Vascular Tree: Segmentation and Estimation Methods. Arquivos Brasileiros de Oftalmologia, 70, 413--422 (2007)
35. Ţălu, Ş., Vlăduţiu, C., Popescu, L. A., Lupaşcu, C. A., Vesa, Ş. C., Ţălu, S. D.: Fractal and Lacunarity Analysis of Human Retinal Vessel Arborisation in Normal and Amblyopic eyes. HVM Bioflux, 5, 45--51 (2013)
36 Liew, G., Wang, J. J., Cheung, N., Zhang, Y. P., Hsu, W., Lee, M. L., Mitchell, P., Tikellis, G., Taylor, B., Wong, T. Y.: The Retinal Vasculature As a Fractal: Methodology, Reliability and Relationship to Blood Pressure. Ophthalmology, 115, 1951--1956 (2008)
37. Ţălu, Ş., Ţălu, S. D., Giovanzana, S., Ţălu, M. Petrescu-Mag, I. V.: Monofractal and Multifractal Analysis in Human Retinal Pathology. In 6th EOS Topical Meeting on Visual and Physiological Optics, Dublin, Ireland, 77-78 (2012)
38. Avakian, A., Kalina, R. E., Sage, E. H., Rambhia, A. H.,.Elliott, K. E., Chuang, E. L.: Fractal Analysis of Region-based Vascular Change in the Normal and Non-proliferative Diabetic Retina. Current Eye Research, 24, 274--280 (2002)
39. Ţălu, Ş., Fazekas, Z., Ţălu, M., Giovanzana, S.: Multifractal Analysis of Human Peripapillary Atrophy. Proceedings of 8th International Symposium on Image and Signal Processing and Analysis, Trieste, Italy, 698--703, (2013)

40. Lázár, I., Hajdu, A.: Segmentation of Retinal Vessels by Means of Directional Response Vector Similarity and Region Growing. Under review by International Journal of Biomedical Imaging; submitted to the journal in (2014)

41. Lowell, J., Hunter, A., Steel, D., Basu, A., Ryder, R., Kennedy, R. L.: Measurement of Retinal Vessel Widths from Fundus Images Based on 2-D Modeling. IEEE Transactions on Medical Imaging, 23, 1196--1204 (2004)

42. Al-Diri, B., Hunter, A., Steel, D.: An Active Contour Model for Segmenting and Measuring Retinal Vessels. IEEE Transactions on Medical Imaging, 28, 1488--1497 (2009)

43. Ricci E., Perfetti, R.: Retinal Blood Vessel Segmentation Using Line Operators and Support Vector Classification. IEEE Transactions on Medical Imaging, 26, 1357--1365 (2007)

44. Kharghanian, R., Ahmadyfard, A.: Retinal Blood Vessel Segmentation Using Gabor Wavelet and Line Operator. International Journal of Machine Learning and Computing, 2, 593--597 (2012)

45. Kovács, Gy., Hajdu, A.: Template Matching Based Segmentation of Retinal Vessels Using Generalized Gabor Functions. Under review by Medical Image Analysis; submitted to the journal in: (2013)

46. Lupaşcu, C. A.: Unsupervised Segmentation of Retinal Vessels. MSc thesis, University of Palermo, Italy, 1--87 (2011)

47. Călugăru D, Călugăru, M.: Intravitreal Bevacizumab in Acute Central/Hemi-central Retinal Vein Occlusions: Three-Year Results of a Prospective Clinical Study. Published online before the printed version, Journal of Ocular Pharmacology and Therapeutics, (2014)

48. Rasband, W.: Image J software (Version ImageJ 1.48g), National Institutes of Health, Bethesda, MD, USA. Available from: http://imagej.nih.gov/ij (accessed in 2014)

49. Karperien, A. FracLac (Version 2.5) for Image J software, Charles Stuart University, Australia, available from: http://rsbweb.nih.gov/ij/plugins/fraclac/FLHelp/Introduction.htm. Accessed in 2014.

50. Falconer, K.: Fractal Geometry: Mathematical Foundations and Applications, John Wiley & Sons Ltd, UK, 43--45 (2003)

51. DRIVE: Digital Retinal Images for Vessel Extraction, http://www.isi.uu.nl/Research/Databases/ DRIVE/ Accessed in 2014.

52. STructured Analysis of the REtina, http://www.ces.clemson.edu/~ahoover/stare/ Accessed in 2014.

53. High-Resolution Fundus Image Database, https://www5.cs.fau.de/research/data/fundus-images/ Accessed in 2014.